

ZIPFORMER: A FASTER AND BETTER ENCODER FOR AUTOMATIC SPEECH RECOGNITION

Zengwei Yao, Liyong Guo, Xiaoyu Yang, Wei Kang, Fangjun Kuang,
Yifan Yang, Zengrui Jin, Long Lin, Daniel Povey
Xiaomi Corp., Beijing, China
dpovey@xiaomi.com

ABSTRACT

The Conformer has become the most popular encoder model for automatic speech recognition (ASR). It adds convolution modules to a Transformer to learn both local and global dependencies. In this work we describe a faster, more memory-efficient, and better-performing Transformer, called Zipformer. Modeling changes include: 1) a U-Net-like encoder structure where middle stacks operate at lower frame rates; 2) reorganized block structure with more modules, within which we re-use attention weights for efficiency; 3) a modified form of LayerNorm called BiasNorm allows us to retain some length information; 4) new activation functions SwooshR and SwooshL work better than Swish. We also propose a new optimizer, called ScaledAdam, which scales the update by each tensor’s current scale to keep the relative change about the same, and also explicitly learns the parameter scale. It achieves faster convergence and better performance than Adam. Extensive experiments on LibriSpeech, Aishell-1, and WenetSpeech datasets demonstrate the effectiveness of our proposed Zipformer over other state-of-the-art ASR models. Our code is publicly available at <https://github.com/k2-fsa/icefall>.

1 INTRODUCTION

End-to-end models have achieved remarkable success in automatic speech recognition (ASR). An effective encoder architecture that performs temporal modeling on the speech sequence plays a vital role in end-to-end ASR models. A most prominent example is Conformer (Gulati et al., 2020), which combines the advantages of the convolutional neural network (CNN) models (Zhang et al., 2017; Li et al., 2019; Kriman et al., 2020) and Transformer models (Dong et al., 2018; Karita et al., 2019; Zhang et al., 2020b). By integrating CNN into Transformer (Vaswani et al., 2017), Conformer is able to extract both local and global dependencies on speech sequences, and achieves state-of-the-art performance in ASR.

In this work, we propose a faster, more memory-efficient, and better-performing Transformer as ASR encoder, called *Zipformer*. First, unlike Conformer that operates on the sequence at a constant frame rate, *Zipformer* adopts a U-Net-like (Ronneberger et al., 2015) structure, which consists of multiple stacks downsampling the sequence to various lower frame rates. Second, we re-design the block structure, which is equipped with more modules like two Conformer blocks, and reuses the attention weights for efficiency. We propose *BiasNorm* as a simpler replacement of LayerNorm, which allows for retaining length information in normalization. We also replace Swish with our new activation functions *SwooshR* and *SwooshL* to achieve better results. In addition, we devise a parameter-scale-invariant version of Adam, called *ScaledAdam*, which scales the update by the current parameter scale and also explicitly learns the parameter scale. Compared to Adam, *ScaledAdam* enables faster convergence and better performance.

Extensive experiments are conducted on LibriSpeech, Aishell-1, and WenetSpeech datasets, and results demonstrate the effectiveness of the proposed modeling and optimization-related innovations. *Zipformer* achieves state-of-the-art results on all three datasets. It is worth mentioning that *Zipformer* is the first model ever to achieve results comparable to those reported in the Conformer paper on the LibriSpeech dataset (these results have proved difficult for others to reproduce). In terms of efficiency, *Zipformer* converges faster during training and speeds up the inference by more than

50% compared to previous studies while requiring less GPU memory. We perform detailed ablation studies to investigate the contribution of individual components.

2 RELATED WORK

Model architecture. Deep convolution architectures have been applied to end-to-end ASR (Zhang et al., 2017; Li et al., 2019). Follow-up works explore improvements by using depthwise separable convolutions (Howard et al., 2017) for efficiency (Kriman et al., 2020), and incorporating squeeze-and-excitation module (Hu et al., 2018) to capture longer context (Han et al., 2020). Inspired by the success of Transformer (Vaswani et al., 2017) in natural language processing (NLP) field, some works adapt Transformer to speech applications (Dong et al., 2018; Karita et al., 2019; Zhang et al., 2020b; Wang et al., 2020; Zhang et al., 2020a). Compared to CNN, the remarkable benefit of Transformer is that it can learn global dependencies based on self-attention, which is essential for speech processing task. By integrating convolution into Transformer, Conformer (Gulati et al., 2020) gains powerful capability of modeling both local and global contextual information, and outperforms all previous ASR models.

Recent works explore architecture changes on Conformer to further reduce the computational cost and improve the recognition performance. Squeezeformer (Kim et al., 2022) adopts a temporal U-Net structure in which the middle modules operate at half frame rates, and also redesigns the block structure to make it similar to the standard Transformer block (Vaswani et al., 2017). Branchformer (Peng et al., 2022) incorporates parallel branches to model various ranged context, in which one branch captures the local context with convolutional gating multi-layer perceptron (MLP), while the other branch learns long-range dependencies with self-attention. E-Branchformer (Kim et al., 2023) further improves Branchformer by enhancing the branch merging mechanism by convolution-based module.

Zipformer shares similar ideas about temporal downsampling as the previous work Squeezeformer. However, compared to the fixed downsampling ratio in Squeezeformer, *Zipformer* operates at different downsampling ratios at different encoder stacks and uses much more aggressive downsampling ratios in the middle encoder stacks. In addition to the modeling differences, our work also focuses on optimization-related changes including a new optimizer *ScaledAdam*, which are shown to improve convergence in the experiments.

End-to-end framework. Connectionist temporal classification (CTC) (Graves et al., 2006) is one of the earliest frameworks for end-to-end ASR, but its performance is limited by the frame independent assumption. To this end, a hybrid architecture that integrates attention-based encoder-decoder (AED) (Chan et al., 2015) in CTC (Watanabe et al., 2017) (CTC/AED) is proposed to improve the performance. Neural transducer (Graves, 2012), commonly known as RNN-T, addresses the frame independence assumption using a label decoder and a joint network and becomes a popular framework due to its superior performance. Recently, various approaches such as pruning (Kuang et al., 2022; Wang et al., 2023; Mahadeokar et al., 2021) or batch-splitting (Kuchaiev et al., 2019) are proposed to accelerate the training speed and reduce memory usage of neural transducers.

3 METHOD

3.1 DOWNSAMPLED ENCODER STRUCTURE

Figure 1 presents the overall architecture of the proposed *Zipformer* model. Different from Conformer (Gulati et al., 2020) that processes the sequence at a fixed frame rate of 25Hz, *Zipformer* uses a U-Net-like structure learning temporal representation at different resolutions in a more efficient way. Specifically, given the acoustic features with frame rate of 100Hz, the convolution-based module called *Conv-Embed* first reduces the length by a factor of 2, resulting in a 50Hz embedding sequence. The obtained sequence is then fed into 6 cascaded stacks to learn temporal representation at frame rates of 50Hz, 25Hz, 12.5Hz, 6.25Hz, 12.5Hz, and 25Hz, respectively. Except for the first stack, the other stacks all adopt the downsampled structures, processing the sequence at lower frame rates. The frame rate between stacks is consistently 50Hz. Different stacks have different embedding dimensions, and the middle stacks have larger dimensions. The output of each stack is truncated or padded with zeros to match the dimension of the next stack. The final encoder output dimension is set to the maximum of all stacks’ dimensions. Specifically, if the last stack output has the largest dimension, it is taken as the encoder output; otherwise, it is concatenated from differ-

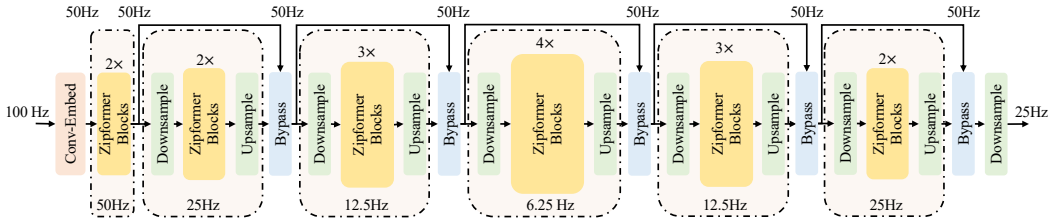


Figure 1: Overall architecture of Zipformer.

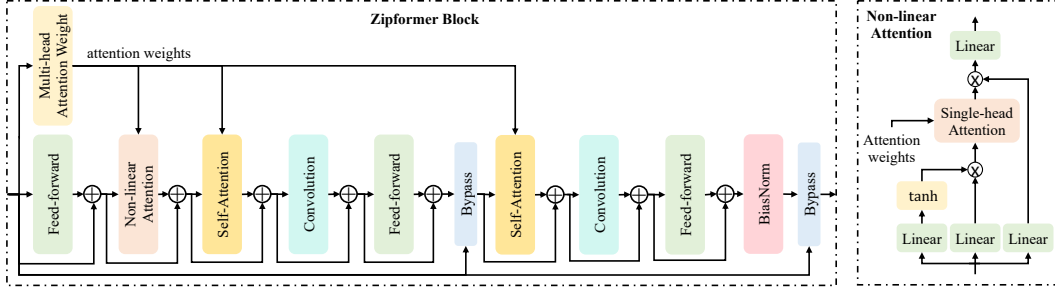


Figure 2: (Left): Zipformer block structure. (Right): Non-Linear Attention module structure.

ent pieces of stack outputs, taking each dimension from the most recent output that has it present. Finally, a *Downsample* module converts the sequence to 25Hz, resulting in the encoder output.

Conv-Embed. In *Conv-Embed* we use three 2-D convolutional layers with time \times frequency strides of 1×2 , 2×2 , and 1×2 , and output channels of 8, 32, and 128, respectively. Subsequently, we utilize one ConvNeXt layer (Liu et al., 2022) similar to Nextformer (Jiang et al., 2022), which is composed of a depth-wise convolution with kernel size of 7×7 , a point-wise convolution with 384 output channels, a *SwooshL* activation function (described in Section 3.4), and a point-wise convolution with 128 output channels. Residual connection is applied on the ConvNeXt module. Finally, a linear layer followed by a *BiasNorm* (described in Section 3.3) is used to adjust the feature dimension to match the first stack.

Downsampled stacks. In the downsampled stacks, the pairwise *Downsample* and *Upsample* modules perform symmetric scaling down and scaling up in sequence length, respectively, using almost the simplest methods. For example, with a factor of 2, the *Downsample* module averages every 2 frames with 2 learnable scalar weights (after softmax normalization), and the *Upsample* module just repeats each frame twice. After downsampling, it employs the stacking *Zipformer* blocks (described in Section 3.2) for temporal modeling at lower frame rates. Finally, it utilizes the *Bypass* module (described in Section 3.2) to combine the stack input and stack output in a learnable way.

3.2 ZIPFORMER BLOCK

Conformer block consists of four modules: feed-forward, Multi-Head Self-Attention (MHSA), convolution, and feed-forward. MHSA learns global context by two steps: computing attention weights using the dot-product operation and aggregating different frames with these attention weights. However, MHSA typically accounts for a large computational cost, since above two steps both require quadratic complexity with respect to the sequence length. Hence, we decompose MHSA into two individual modules according to above two steps: Multi-Head Attention Weight (*MHAW*) and Self-Attention (*SA*). This change allows to perform the attention computation twice more efficiently in each block by using one *MHAW* module and two *SA* modules. In addition, we propose a new module called Non-Linear Attention (*NLA*) to make full use of the computed attention weights to capture the global information.

As illustrated in Figure 2 (Left), *Zipformer* block is equipped with about twice the depth of the Conformer block (Gulati et al., 2020). The main motivation is to allow the re-use of the attention weights to save time and memory. Specifically, the block input is first fed into an *MHAW* module, which calculates the attention weights and shares them with an *NLA* module and two *SA* modules. Meanwhile, the block input is also fed into a feed-forward module followed by the *NLA* module.

Then it applies two module groups, each consisting of *SA*, convolution, and feed-forward. Finally, a *BiasNorm* (described in Section 3.3) is used to normalize the block output. In addition to the regular residual connections using adding operation, each block utilizes two *Bypass* modules to combine the block input and the module outputs, placed in the middle and end of the block. Note that different from regular Transformer models (Vaswani et al., 2017), we don’t use normalization layer such as LayerNorm (Ba et al., 2016) for each module to periodically prevent activations from becoming either too large or too small, since our proposed *ScaledAdam* optimizer is able to learn the parameter scales (described in Section 3.5).

Non-Linear Attention. Figure 2 (Right) presents the *NLA* structure. It also leverages the pre-computed attention weights from *MHAW* to aggregate the embedding vectors over the time axis, which is similar to *SA*. Specifically, it first projects the input with 3 linear layers to *A*, *B*, and *C*, each being of 3/4 input dimension. The module output is $\text{linear}(A \odot \text{attention}(\tanh(B) \odot C))$, where \odot denotes the element-wise multiplication, attention represents matrix-multiplying on the time axis by a single head of previously computed attention weights, and the linear layer recovers the dimension to the same as the input.

Bypass. The *Bypass* module learns channel-wise scalar weights \mathbf{c} to combine the module input \mathbf{x} and module output \mathbf{y} : $(1 - \mathbf{c}) \odot \mathbf{x} + \mathbf{c} \odot \mathbf{y}$. In training, we initially limit the values of \mathbf{c} in range of $[0.9, 1.0]$ and then change the minimum to 0.2 after 20000 steps. We found that making modules “straight-through” at the beginning (i.e. allowing very little bypass) helps model convergence..

3.3 BIASNORM

Conformer (Gulati et al., 2020) utilizes LayerNorm (Ba et al., 2016) to normalize the module activations. Given \mathbf{x} with D channels, LayerNorm is formulated as:

$$\text{LayerNorm}(\mathbf{x}) = \frac{\mathbf{x} - \mathbb{E}[\mathbf{x}]}{\sqrt{\text{Var}[\mathbf{x}] + \epsilon}} \odot \gamma + \beta. \quad (1)$$

Specifically, it first computes the mean $\mathbb{E}[\mathbf{x}]$ and the standard-deviation $\sqrt{\text{Var}[\mathbf{x}]}$ for normalizing, scaling the vector length to \sqrt{D} . Then it uses the learnable channel-wise scale γ and bias β for transformation, which helps to adjust the size of activations and balance the relative contributions of specific modules. However, we observe that the trained Conformer using LayerNorm suffers from two problems: 1) It sometimes sets one channel to a large constant value, e.g. 50. We argue that it aims to “defeat” the LayerNorm which fully removes the vector length, functioning as a very large value so that length information could be retained after normalization. 2) Some modules (typically feed-forward or convolution) are “dead” as they have extremely small output values, e.g., 10^{-6} . We argue that early in training, the un-trained modules are not useful so they are “turned off” by the LayerNorm scale γ approaching zero. If the scale γ oscillates around zero, the inconsistent sign constantly reverses the gradient directions back-propagating to the modules. Because of the inconsistent gradient sign, the modules never learn anything useful, since this is a bad local optimum which is hard to escape because of the dynamics of stochastic gradient descent-like updates.

To address above problems, we propose the *BiasNorm* which is intended to be a simpler replacement of LayerNorm. Specifically, *BiasNorm* is formulated as:

$$\text{BiasNorm}(\mathbf{x}) = \frac{\mathbf{x}}{\text{RMS}[\mathbf{x} - \mathbf{b}]} \cdot \exp(\gamma), \quad (2)$$

where \mathbf{b} is the learnable channel-wise bias, $\text{RMS}[\mathbf{x} - \mathbf{b}]$ is the root-mean-square value taken over channels, and γ is a scalar. We first remove the operation of mean subtraction since it is a waste of time unless it follows a non-linearity. The bias \mathbf{b} serves as the large constant value which allows to retain the vector length information after normalization. Since the scale $\exp(\gamma)$ is always positive, it avoids the gradient oscillation problem.

3.4 SWOOSHR AND SWOOSHL ACTIVATION FUNCTIONS

Conformer (Gulati et al., 2020) adopts Swish (Ramachandran et al., 2017) activation function with the following formula:

$$\text{Swish}(x) = x \cdot (1 + \exp(-x))^{-1}. \quad (3)$$

In this work, we propose two new activation functions respectively called *SwooshR* and *SwooshL* as replacements of Swish:

$$\begin{aligned} \text{SwooshR}(x) &= \log(1 + \exp(x - 1)) - 0.08x - 0.313261687, \\ \text{SwooshL}(x) &= \log(1 + \exp(x - 4)) - 0.08x - 0.035. \end{aligned} \quad (4)$$

In *SwooshR*, the offset 0.313261687 is to make it pass through the origin; in *SwooshL*, the offset 0.035 was tuned, which slightly outperformed the value exactly making the curve pass through the origin. We present the curves of Swish, *SwooshR*, and *SwooshL* in Appendix Section A.2. *SwooshL* is roughly a right shifted version of *SwooshR*. Note that the suffix ‘‘L’’ or ‘‘R’’ represents whether the left or right zero-crossing is at or around $x = 0$. Similar to Swish, *SwooshR* and *SwooshL* have lower bounds and are non-monotonic. Compared to Swish, the most striking difference is that *SwooshR* and *SwooshL* have non-vanishing slopes for negative inputs, which helps to escape from situations where the input is always negative and prevents the denominator term in Adam-type updates from getting dangerously small. When replacing Swish with *SwooshR*, we observe that the modules with bypass connections, such as feed-forward and ConvNeXt, tend to learn a large negative bias in the preceding linear layer to learn ‘‘normally-off’’ behavior. Therefore, we use *SwooshL* for these ‘‘normally-off’’ modules and use *SwooshR* for convolution modules and the rest of *Conv-Embed*.

3.5 SCALEDADAM OPTIMIZER

We propose a parameter-scale-invariant version of Adam (Kingma & Ba, 2014) called *ScaledAdam*, which enables faster convergence and better performance. *ScaledAdam* scales each parameter’s update proportional to the scale of that parameter, and also explicitly learns the parameter scale. Algorithm 1 in Appendix Section A.1.1 presents the pseudo-code of the *ScaledAdam*.

Let $f(\theta)$ be the loss function that we aim to minimize, which is differentiable w.r.t. the learnable parameter θ . At each step t , Adam computes the parameter gradient $\mathbf{g}_t = \nabla_{\theta} f(\theta_{t-1})$, and updates the first moment $\mathbf{m}_t = \beta_1 \cdot \mathbf{m}_{t-1} + (1 - \beta_1) \cdot \mathbf{g}_t$ and the second moment $\mathbf{v}_t = \beta_2 \cdot \mathbf{v}_{t-1} + (1 - \beta_2) \cdot \mathbf{g}_t^2$ of gradients, where $\beta_1, \beta_2 \in [0, 1)$ are coefficients used to compute the moving averages. The parameter update Δ_t at step t is formulated as:

$$\Delta_t = -\alpha_t \cdot \frac{\sqrt{1 - \beta_2^t}}{1 - \beta_1^t} \cdot \frac{\mathbf{m}_t}{\sqrt{\mathbf{v}_t} + \epsilon}, \quad (5)$$

where α_t is the learning rate typically specified by an external schedule, $\frac{\sqrt{1 - \beta_2^t}}{1 - \beta_1^t}$ is the bias-correction term, and $\epsilon = 10^{-8}$. Whilst Adam is invariant to gradient scale of each parameter, we argue that it still suffers from two limitations: 1) The update Δ_t in Equation 5 does not take into account the parameter scale (denoted as r_{t-1}). Considering the relative parameter change Δ_t/r_{t-1} , Adam might cause learning in relative terms too slowly for parameters with large scales, or too fast for parameters with small scales. 2) It is difficult to learn the parameter scale directly, as the direction of growing or shrinking the parameter tensor is a very specific direction in a large-dimensional space. It’s particularly difficult to shrink a parameter, since each gradient step \mathbf{g}_t adds noise which tends to grow the parameter norm.

Scaling update. To keep the relative change Δ_t/r_{t-1} over parameters of varying scales about the same, we scale the update Δ_t in Equation 5 by the parameter scale r_{t-1} :

$$\Delta'_t = -\alpha_t \cdot r_{t-1} \cdot \frac{\sqrt{1 - \beta_2^t}}{1 - \beta_1^t} \cdot \frac{\mathbf{m}_t}{\sqrt{\mathbf{v}_t} + \epsilon}. \quad (6)$$

We compute the parameter scale r_{t-1} as the root-mean-square value $\text{RMS}[\theta_{t-1}]$. Because the ScaledAdam update is less prone to divergence than Adam, we use a learning rate schedule called *Eden* that does not have a long warm-up period; we also use absolutely larger learning rate values because the parameter RMS value is normally much less than one.

Learning parameter scale. To explicitly learn the parameter scale, we treat it as a regular parameter to be learned, as if we have factored each parameter as $\theta = r \cdot \theta'$, and we are doing gradient descent on the parameter scale r and the underlying parameter θ' . Let h be the gradient of the parameter scale r , at step t we get $h_t = \nabla_r f(\theta_{t-1}) = \mathbf{g}_t \cdot \theta'_{t-1}$. Since Adam is nearly invariant to changes in the gradient scale, for simplicity we replace this with $h_t = \mathbf{g}_t \cdot (r_{t-1} \odot \theta'_{t-1}) = \mathbf{g}_t \cdot \theta_{t-1}$. Following the Adam algorithm, we maintain the first moment $n_t = \beta_1 \cdot n_{t-1} + (1 - \beta_1) \cdot h_t$ and the second moment $w_t = \beta_2 \cdot w_{t-1} + (1 - \beta_2) \cdot h_t^2$ of the scale gradients h_t . The parameter change on θ caused

by updating parameter scale from r_{t-1} to r_t is $\Delta'_{t,r} = (r_t - r_{t-1}) \odot \theta'_{t-1}$. Similar to Equation 6, we also integrate the parameter scale r_{t-1} into the update $\Delta'_{t,r}$:

$$\begin{aligned} \Delta'_{t,r} &= -\eta \cdot \alpha_t \cdot r_{t-1} \cdot \frac{\sqrt{1-\beta_2^t}}{1-\beta_1^t} \cdot \frac{n_t}{\sqrt{w_t + \epsilon}} \odot \theta'_{t-1} \\ &= -\eta \cdot \alpha_t \cdot \frac{\sqrt{1-\beta_2^t}}{1-\beta_1^t} \cdot \frac{n_t}{\sqrt{w_t + \epsilon}} \odot \theta_{t-1}. \end{aligned} \quad (7)$$

where η is a scaling factor on learning rate α_t , and we found that setting $\eta = 0.1$ helps to stabilize the training. Now the update Δ'_t is replaced with $\Delta'_{t,r} + \Delta'_t$, which amounts to adding an extra gradient term in the direction of growing or shrinking each parameter. This also allows to simplify the network structure by removing most of normalization layers in our *Zipformer* Block (described in Section 3.2), since the modules now can easily learn to scale the activations in a suitable range. One similar method called weight normalization (Salimans & Kingma, 2016) decouples the parameter norm from its direction to speed up the convergence. It replaces each parameter with two parameters, respectively specifying the direction and the magnitude. However, ScaledAdam learns the parameter scales by adding an extra update term $\Delta'_{t,r}$, which makes writing the modeling code simpler.

Eden schedule. The proposed *Eden* learning rate schedule is formulated as:

$$\alpha_t = \alpha_{\text{base}} \cdot \left(\frac{t^2 + \alpha_{\text{step}}^2}{\alpha_{\text{step}}^2} \right)^{-0.25} \cdot \left(\frac{e^2 + \alpha_{\text{epoch}}^2}{\alpha_{\text{epoch}}^2} \right)^{-0.25} \cdot \text{linear}(\alpha_{\text{start}}, t_{\text{warmup}}, t). \quad (8)$$

Herein, t is the step index, e is the epoch index, α_{step} and α_{epoch} respectively control the number of steps and number of epochs after which we start significantly decreasing the learning rate, $\text{linear}(\alpha_{\text{start}}, t_{\text{warmup}}, t)$ is a warmup scale increasing linearly from α_{start} to 1 over t_{warmup} steps and then staying constant at 1, α_{base} is the maximum value when setting $\alpha_{\text{start}} = 1$, $\alpha_{\text{warmup}} = 0$. The reason for making *Eden* dependent on both the step index t and the epoch index e is to keep the amount of parameter change after certain amount of training data (e.g., one hour) approximately constant when we change the batch size, so the schedule parameters should not have to be re-tuned if we change the batch size. Other versions of *Eden* replace the ‘‘epoch’’ parts of the formula with some suitable measure of the amount of data seen. In this work, we use $\alpha_{\text{base}} = 0.045$, $\alpha_{\text{start}} = 0.5$, and $t_{\text{warmup}} = 500$.

Efficient implementation. To speedup the optimization in *ScaledAdam*, we group the parameters into batches according to their shape and perform the computation batch by batch. Note that this doesn’t affect the outcome. *ScaledAdam* just requires a little more memory than Adam to cache the gradient moments n_t and w_t (in Equation 7) for the parameter scales.

4 EXPERIMENTS

4.0.1 EXPERIMENTAL SETUP

Architecture variants. We build our *Zipformer* variants with three model scales: small (*Zipformer-S*), medium (*Zipformer-M*), and large (*Zipformer-L*). For the 6 encoder stacks, the numbers of attention heads are set to $\{4,4,4,8,4,4\}$, the convolution kernel sizes are set to $\{31,31,15,15,15,31\}$. In each attention head, the query dimension and value dimension are set to 32 and 12, respectively. For the three feed-forward modules in each *Zipformer* block, the hidden dimensions in the first one and the last one are 3/4 and 5/4 of that in the middle one. We adjust the layers numbers, the embedding dimensions, and the hidden dimensions of the middle feed-forward in each stack to obtain different model scales:

Table 1: Configuration of *Zipformer* at three different scales.

Scale	layer-numbers	embedding-dimensions	feed-forward-dimensions
S	$\{2,2,2,2,2,2\}$	$\{192,256,256,256,256,256\}$	$\{512,768,768,768,768,768\}$
M	$\{2,2,3,4,3,2\}$	$\{192,256,384,512,384,256\}$	$\{512,768,1024,1536,1024,768\}$
L	$\{2,2,4,5,4,2\}$	$\{192,256,512,768,512,256\}$	$\{512,768,1536,2048,1536,768\}$

Datasets. We perform experiments to compare our *Zipformer* with state-of-the-other models on three open-source datasets: 1) LibriSpeech (Panayotov et al., 2015) which consists of about 1000

hours of English audiobook reading; 2) Aishell-1 (Bu et al., 2017) which contains 170 hours of Mandarin speech; 3) WenetSpeech (Zhang et al., 2022a) which consists of 10000+ hours of multi-domain Mandarin speech.

Implementation details. We use Lhotse (Želasko et al., 2021) toolkit for speech data preparation. The model inputs are 80-dimension Mel filter-bank features extracted on 25ms frames with frame shift of 10ms. Speed perturbation (Ko et al., 2015) with factors of 0.9, 1.0, and 1.1 is used to augment the training data. SpecAugment (Park et al., 2019) is also applied during training. We use mixed precision training for our *Zipformer* models. We also employ the activation constraints including *Balancer* and *Whitener* to ensure training consistency and stability. The details of *Balancer* and *Whitener* are presented in Appendix Section A.3. Pruned transducer (Kuang et al., 2022), a memory-efficient version of transducer loss that prunes path with minor posterior is used as the training objective. During decoding, beam search of size 4 with the constraint of emitting at most one symbol per frame is employed (Kang et al., 2023). We don’t use external language models for rescoring, since in this work we focus on improving the encoder model. We employ word-error-rate (WER) and character error rate (CER) as evaluation metric for English and Mandarin datasets, respectively. By default, all of our models are trained on 32GB NVIDIA Tesla V100 GPUs. For LibriSpeech dataset, *Zipformer-M* and *Zipformer-L* are trained for 50 epochs on 4 GPUs, and *Zipformer-S* is trained for 50 epochs on 2 GPUs. For Aishell-1 dataset, our models are trained for 56 epochs on 2 GPUs. For WenetSpeech dataset, our models are trained for 14 epochs on 4 GPUs.

4.0.2 COMPARISON WITH STATE-OF-THE-ART MODELS

In this section, we compare the proposed *Zipformer* with other state-of-the-art models.

LibriSpeech dataset. Table 2 shows the results on LibriSpeech test datasets for *Zipformer* and other state-of-the-art models. For Conformer, we also list the WERs reproduced by us and other open-source frameworks. Note that there is a performance gap between the open-source reproduced Conformer and the original Conformer. Our *Zipformer-S* model achieves lower WERs than all variants of Squeezeformer while having much fewer parameters and floating point operations (FLOPs). Our *Zipformer-L* outperforms Squeezeformer-L, Branchformer and our reproduced Conformer-L by a large margin while saving over 50% FLOPs. Noticeably, when trained on 8 80G NVIDIA Tesla A100 GPUs for 170 epochs, *Zipformer-L* achieves WERs of 2.00%/4.38% with sufficient computing resources (last row), which is the first model to approach Conformer-L to the best of our knowledge.

We also compare the speed and memory usage between the proposed *Zipformer* and other state-of-the-art models. Figure 3 presents the comparison results in terms of averaged inference time and peak memory usage in inference mode for batches of 30-second audios on an NVIDIA Tesla V100 GPU. The batch size is set to 30 to ensure all models do not have out of memory problems during inference. In overall, *Zipformer* models achieves better trade-off between performance and efficiency than other models. Especially for the large scale, *Zipformer-L* requires much less computation time and memory than other counterparts.

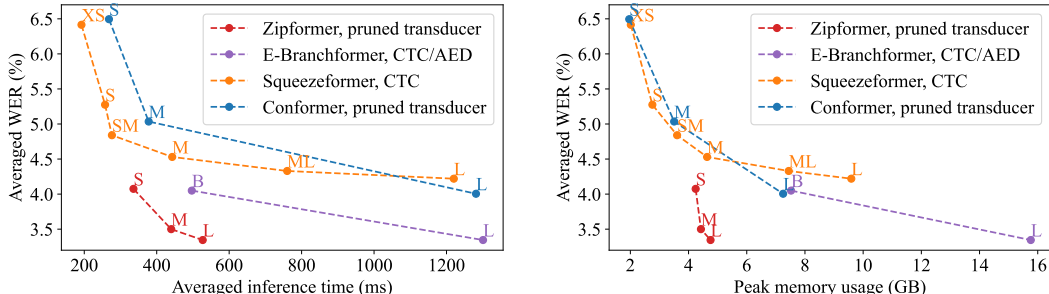


Figure 3: (Left) Averaged inference time and (Right) peak memory usage vs. WER comparison for different models. The WER is averaged on LibriSpeech *test-clean* and *test-other*. Averaged inference time and peak memory usage are reported for the **encoders** in inference mode for batches of 30-second audios with batch size of 30 on a single NVIDIA Tesla V100 GPU.

Aishell-1 dataset. Table 3 shows the CERs on Aishell-1 dataset. Compared to the Conformer model implemented in ESPnet toolkit, our *Zipformer-S* achieves better performance with fewer parameters. Scaling up the model leads to lower WERs, and *Zipformer-M/L* outperform all other models.

Table 2: WER(%) comparison between different models on LibriSpeech dataset. We also include the number of parameters and FLOPs of encoder for a 30s input audio measured with DeepSpeed (Rasley et al., 2020). *Trained with 8 80G NVIDIA Tesla A100 GPUs for 170 epochs.

Model	Type	Params (M)	GFLOPs	test-clean (%)	test-other (%)
Squeezeformer-XS (Kim et al., 2022)	CTC	9.0	18.2	3.74	9.09
Squeezeformer-S (Kim et al., 2022)	CTC	18.6	33.7	3.08	7.47
Squeezeformer-SM (Kim et al., 2022)	CTC	28.2	47.6	2.79	6.89
Squeezeformer-M (Kim et al., 2022)	CTC	55.6	88.4	2.56	6.50
Squeezeformer-ML (Kim et al., 2022)	CTC	125.1	183.3	2.61	6.05
Squeezeformer-L (Kim et al., 2022)	CTC	236.3	333.7	2.47	5.97
E-Branchformer-B (Kim et al., 2023)	CTC/AED	41.1	78.1	2.49	5.61
Branchformer (Peng et al., 2022)	CTC/AED	116.2	238.3	2.4	5.5
E-Branchformer-L (Kim et al., 2023)	CTC/AED	148.9	284.4	2.14	4.55
Conformer-S (Gulati et al., 2020)	transducer	10.3	–	2.7	6.3
Conformer-M (Gulati et al., 2020)	transducer	30.7	–	2.3	5.0
Conformer-L (Gulati et al., 2020)	transducer	118.8	–	2.1	4.3
Conformer in WeNet (Zhang et al., 2022b)	CTC/AED	121.3	–	2.66	6.53
Conformer in ESPnet (Miyazaki et al., 2023)	CTC/AED	113.2	–	2.29	5.13
Conformer-S	pruned transducer	9.8	29.1	3.75	9.24
Conformer-M	pruned transducer	28.4	77.0	2.96	7.11
Conformer-L	pruned transducer	122.5	294.2	2.46	5.55
<i>Zipformer-S</i>	pruned transducer	23.3	40.8	2.42	5.73
<i>Zipformer-M</i>	pruned transducer	65.6	62.9	2.21	4.79
<i>Zipformer-L</i>	pruned transducer	148.4	107.7	2.06	4.63
<i>Zipformer-L*</i>	pruned transducer	148.4	107.7	2.00	4.38

WenetSpeech. Table 4 presents the experimental results on WenetSpeech dataset. Again, our *Zipformer-M* and *Zipformer-L* outperform all other models on *Test_Net* and *Test_Meeting* test sets. With only one third of the parameters, our *Zipformer-S* yields lower WERs than Conformer models.

Table 3: CER(%) comparison between different models on Aishell-1 dataset.

Model	Params (M)	Type	Dev	Test
Conformer in ESPnet (Watanabe et al., 2018)	46.2	CTC/AED	4.5	4.9
Conformer in WeNet (Yao et al., 2021)	46.3	CTC/AED	–	4.61
E-Branchformer in ESPnet (Watanabe et al., 2018)	37.9	CTC/AED	4.2	4.5
Branchformer (Peng et al., 2022)	45.4	CTC/AED	4.19	4.43
<i>Zipformer-S</i>	30.2	pruned transducer	4.4	4.67
<i>Zipformer-M</i>	73.4	pruned transducer	4.13	4.4
<i>Zipformer-L</i>	157.3	pruned transducer	4.03	4.28

Table 4: CER(%) comparison between different models on WenetSpeech dataset.

Model	Params (M)	Type	Dev	Test_Net	Test_Meeting
Conformer in ESPnet (Watanabe et al., 2018)	116.9	CTC/AED	9.70	8.90	15.90
Conformer in WeNet (Yao et al., 2021)	116.9	CTC/AED	8.88	9.70	15.59
Conformer-MoE(16e) (You et al., 2022)	425	CTC/AED, MoE	7.67	8.28	13.96
Conformer-MoE(32e) (You et al., 2022)	–	CTC/AED, MoE	7.49	7.99	13.69
Conformer-MoE(64e) (You et al., 2022)	–	CTC/AED, MoE	7.19	8.36	13.72
<i>Zipformer-S</i>	32.3	pruned transducer	7.96	8.6	13.97
<i>Zipformer-M</i>	75.9	pruned transducer	7.32	7.61	12.35
<i>Zipformer-L</i>	160.9	pruned transducer	7.29	7.24	12.06

4.0.3 ABLATION STUDIES

We perform ablation experiments on LibriSpeech dataset to investigate the effect of each proposed functional technique. With *Zipformer-M* as the base model, we make one change each time while keeping the others untouched. Table 5 presents the experimental results.

Encoder structure. We remove the temporal downsampling structure from *Zipformer* and use *Conv-Embed* with downsampling rate of 4 like Conformer. The resulting model has 12 *Zipformer* blocks with a constant embedding dimension of 512 and has more parameters than the base model.

Table 5: Ablation studies for *Zipformer*-M, including encoder structure, block structure, normalization layer, activation function and optimizer.

Ablation	Params (M)	test-clean (%)	test-other (%)
<i>Zipformer</i> -M	65.6	2.21	4.79
Encoder structure			
No temporal downsampling	94.2	2.23	5.09
Block structure			
Double Conformer-style blocks	73.9	2.18	4.95
No <i>NLA</i>	58.7	2.16	4.97
No <i>NLA</i> , no attention weights sharing	60.9	2.20	5.10
No <i>Bypass</i>	65.5	2.25	4.86
Normalization layer			
LayerNorm	65.6	2.29	4.97
Activation function			
Only <i>SwooshR</i>	65.5	2.32	5.21
Swish	65.5	2.27	5.37
Optimizer			
Adam	65.6	2.38	5.51

Experimental results in Table 5 show that the resulting model without the downsampled structure yields higher WERs on both test set. It indicates that the temporal downsampling structure for efficiency does not cause information loss, but facilitates the modeling capacity with less parameters.

Block structure. As each *Zipformer* block has roughly twice modules as a Conformer block, we replace each *Zipformer* block in the base model with two Conformer blocks stacked together. This leads to 0.16% absolute WER reduction on *test-other* even with a larger model size, suggesting the benefits of *Zipformer* block structure. Removing either *NLA* or *Bypass* leads to performance degradation. If we further remove the attention weights sharing mechanism after removing *NLA*, the model has slightly more parameters and slower inference speed, but the WERs are not improved. We hypothesize that the two attention weights inside one *Zipformer* block are quite consistent and sharing them does not harm the model.

Normalization layer. Replacing *BiasNorm* with LayerNorm in *Zipformer* leads to WER drops of 0.08% and 0.18% on *test-clean* and *test-other*, respectively. It indicates the advantage of the proposed *BiasNorm* which allows to retain some length information in normalization.

Activation function. When using only *SwooshR* for all modules in *Zipformer*, the WER drops by 0.11% and 0.42% on *test-clean* and *test-other*, respectively, which validates the effectiveness of particularly using *SwooshL* for the “normally-off” modules. Employing Swish leads to more performance degradation, which indicates the advantage of *SwooshR* over Swish.

Optimizer. When using Adam to train *Zipformer*, we have to apply *BiasNorm* for each module in *Zipformer* block to avoid model divergence, since Adam cannot learn the scale of each parameter to adjust the module activations like *ScaledAdam*. We try different learning rate factors (denoted as α_{base}) for *ScaledAdam* (0.025, 0.035, 0.045, 0.055) and Adam (2.5, 5.0, 7.5, 10.0) separately. Following (Gulati et al., 2020), the learning rate schedule for Adam is $\alpha_t = \alpha_{\text{base}} \cdot 512^{-0.5} \cdot \min(t^{-0.5}, t \cdot 10000^{-1.5})$. Figure A.2 in Appendix Section A.1.2 presents the averaged WERs on *test-clean* and *test-other* at different epochs as well as the learning rates at different steps. We show the best results of *ScaledAdam* with $\alpha_{\text{base}} = 0.045$ and Adam with $\alpha_{\text{base}} = 7.5$ in Table 5. *ScaledAdam* outperforms Adam by 0.17% and 0.72% on *test-clean* and *test-other*, respectively. The results indicate that *ScaledAdam* enables faster convergence and better performance than Adam.

5 CONCLUSION

In this work, we present the *Zipformer*, which serves as an efficient ASR encoder. It has an U-Net-like encoder structure, which downsamples the sequence to various lower frame rates. The re-designed block structure equipped with more modules reuses the computed attention weights for efficiency. It also employs the new normalization method *BiasNorm*, as well as the new activation functions *SwooshR* and *SwooshL*. Meanwhile, the proposed optimizer *ScaledAdam* enables faster convergence and better performance. Extensive experiments on LibriSpeech, Aishell-1 and Wenet-Speech datasets have demonstrated the effectiveness of the proposed *Zipformer*.

REFERENCES

- Jimmy Lei Ba, Jamie Ryan Kiros, and Geoffrey E Hinton. Layer normalization. *arXiv preprint arXiv:1607.06450*, 2016.
- Hui Bu, Jiayu Du, Xingyu Na, Bengu Wu, and Hao Zheng. Aishell-1: An open-source mandarin speech corpus and a speech recognition baseline. In *20th conference of the oriental chapter of the international coordinating committee on speech databases and speech I/O systems and assessment (O-COCOSDA)*, pp. 1–5, 2017.
- William Chan, Navdeep Jaitly, Quoc V Le, and Oriol Vinyals. Listen, attend and spell. *arXiv preprint arXiv:1508.01211*, 2015.
- Linhao Dong, Shuang Xu, and Bo Xu. Speech-transformer: a no-recurrence sequence-to-sequence model for speech recognition. In *IEEE international conference on acoustics, speech and signal processing (ICASSP)*, pp. 5884–5888, 2018.
- Alex Graves. Sequence transduction with recurrent neural networks. *arXiv preprint arXiv:1211.3711*, 2012.
- Alex Graves, Santiago Fernández, Faustino Gomez, and Jürgen Schmidhuber. Connectionist temporal classification: labelling unsegmented sequence data with recurrent neural networks. In *Proceedings of the 23rd international conference on Machine learning*, pp. 369–376, 2006.
- Anmol Gulati, James Qin, Chung-Cheng Chiu, Niki Parmar, Yu Zhang, Jiahui Yu, Wei Han, Shibo Wang, Zhengdong Zhang, Yonghui Wu, and Ruoming Pang. Conformer: Convolution-augmented Transformer for Speech Recognition. In *Proc. Interspeech 2020*, pp. 5036–5040, 2020.
- Wei Han, Zhengdong Zhang, Yu Zhang, Jiahui Yu, Chung-Cheng Chiu, James Qin, Anmol Gulati, Ruoming Pang, and Yonghui Wu. Contextnet: Improving convolutional neural networks for automatic speech recognition with global context. *arXiv preprint arXiv:2005.03191*, 2020.
- Andrew G Howard, Menglong Zhu, Bo Chen, Dmitry Kalenichenko, Weijun Wang, Tobias Weyand, Marco Andreetto, and Hartwig Adam. Mobilenets: Efficient convolutional neural networks for mobile vision applications. *arXiv preprint arXiv:1704.04861*, 2017.
- Jie Hu, Li Shen, and Gang Sun. Squeeze-and-excitation networks. In *Proceedings of the IEEE conference on computer vision and pattern recognition*, pp. 7132–7141, 2018.
- Yongjun Jiang, Jian Yu, Wenwen Yang, Bihong Zhang, and Yanfeng Wang. Nextformer: A convnext augmented conformer for end-to-end speech recognition. *arXiv preprint arXiv:2206.14747*, 2022.
- Wei Kang, Liyong Guo, Fangjun Kuang, Long Lin, Mingshuang Luo, Zengwei Yao, Xiaoyu Yang, Piotr Żelasko, and Daniel Povey. Fast and parallel decoding for transducer. In *ICASSP 2023-2023 IEEE International Conference on Acoustics, Speech and Signal Processing (ICASSP)*, pp. 1–5. IEEE, 2023.
- Shigeki Karita, Nanxin Chen, Tomoki Hayashi, Takaaki Hori, Hirofumi Inaguma, Ziyang Jiang, Masao Someki, Nelson Enrique Yalta Soplín, Ryuichi Yamamoto, Xiaofei Wang, et al. A comparative study on transformer vs rnn in speech applications. In *IEEE Automatic Speech Recognition and Understanding Workshop (ASRU)*, pp. 449–456, 2019.
- Kwangyoun Kim, Felix Wu, Yifan Peng, Jing Pan, Prashant Sridhar, Kyu J Han, and Shinji Watanabe. E-branchformer: Branchformer with enhanced merging for speech recognition. In *2022 IEEE Spoken Language Technology Workshop (SLT)*, pp. 84–91. IEEE, 2023.
- Sehoon Kim, Amir Gholami, Albert Shaw, Nicholas Lee, Karttikeya Mangalam, Jitendra Malik, Michael W Mahoney, and Kurt Keutzer. Squeezeformer: An efficient transformer for automatic speech recognition. *Advances in Neural Information Processing Systems*, 35:9361–9373, 2022.
- Diederik P Kingma and Jimmy Ba. Adam: A method for stochastic optimization. *arXiv preprint arXiv:1412.6980*, 2014.

- Tom Ko, Vijayaditya Peddinti, Daniel Povey, and Sanjeev Khudanpur. Audio augmentation for speech recognition. In *Sixteenth annual conference of the international speech communication association*, 2015.
- Samuel Krman, Stanislav Beliaev, Boris Ginsburg, Jocelyn Huang, Oleksii Kuchaiev, Vitaly Lavrukhin, Ryan Leary, Jason Li, and Yang Zhang. Quartznet: Deep automatic speech recognition with 1d time-channel separable convolutions. In *IEEE International Conference on Acoustics, Speech and Signal Processing (ICASSP)*, pp. 6124–6128, 2020.
- Fangjun Kuang, Liyong Guo, Wei Kang, Long Lin, Mingshuang Luo, Zengwei Yao, and Daniel Povey. Pruned rnn-t for fast, memory-efficient asr training. *arXiv preprint arXiv:2206.13236*, 2022.
- Oleksii Kuchaiev, Jason Li, Huyen Nguyen, Oleksii Hrinchuk, Ryan Leary, Boris Ginsburg, Samuel Krman, Stanislav Beliaev, Vitaly Lavrukhin, Jack Cook, et al. Nemo: a toolkit for building ai applications using neural modules. *arXiv preprint arXiv:1909.09577*, 2019.
- Jason Li, Vitaly Lavrukhin, Boris Ginsburg, Ryan Leary, Oleksii Kuchaiev, Jonathan M Cohen, Huyen Nguyen, and Ravi Teja Gadde. Jasper: An end-to-end convolutional neural acoustic model. *arXiv preprint arXiv:1904.03288*, 2019.
- Zhuang Liu, Hanzi Mao, Chao-Yuan Wu, Christoph Feichtenhofer, Trevor Darrell, and Saining Xie. A convnet for the 2020s. In *Proceedings of the IEEE/CVF conference on computer vision and pattern recognition*, pp. 11976–11986, 2022.
- Jay Mahadeokar, Yuan Shangguan, Duc Le, Gil Keren, Hang Su, Thong Le, Ching-Feng Yeh, Christian Fuegen, and Michael L Seltzer. Alignment restricted streaming recurrent neural network transducer. In *Proc. SLT. IEEE*, 2021.
- Koichi Miyazaki, Masato Murata, and Tomoki Koriyama. Structured state space decoder for speech recognition and synthesis. In *IEEE International Conference on Acoustics, Speech and Signal Processing (ICASSP)*, pp. 1–5, 2023.
- Vassil Panayotov, Guoguo Chen, Daniel Povey, and Sanjeev Khudanpur. Librispeech: an asr corpus based on public domain audio books. In *IEEE international conference on acoustics, speech and signal processing (ICASSP)*, pp. 5206–5210, 2015.
- Daniel S Park, William Chan, Yu Zhang, Chung-Cheng Chiu, Barret Zoph, Ekin D Cubuk, and Quoc V Le. SpecAugment: A simple data augmentation method for automatic speech recognition. *arXiv preprint arXiv:1904.08779*, 2019.
- Yifan Peng, Siddharth Dalmia, Ian Lane, and Shinji Watanabe. Branchformer: Parallel mlp-attention architectures to capture local and global context for speech recognition and understanding. In *International Conference on Machine Learning*, pp. 17627–17643. PMLR, 2022.
- Prajit Ramachandran, Barret Zoph, and Quoc V Le. Searching for activation functions. *arXiv preprint arXiv:1710.05941*, 2017.
- Jeff Rasley, Samyam Rajbhandari, Olatunji Ruwase, and Yuxiong He. Deepspeed: System optimizations enable training deep learning models with over 100 billion parameters. In *Proceedings of the 26th ACM SIGKDD International Conference on Knowledge Discovery & Data Mining*, pp. 3505–3506, 2020.
- Olaf Ronneberger, Philipp Fischer, and Thomas Brox. U-net: Convolutional networks for biomedical image segmentation. In *Medical Image Computing and Computer-Assisted Intervention—MICCAI*, pp. 234–241, 2015.
- Tim Salimans and Durk P Kingma. Weight normalization: A simple reparameterization to accelerate training of deep neural networks. *Advances in neural information processing systems*, 29, 2016.
- Ashish Vaswani, Noam Shazeer, Niki Parmar, Jakob Uszkoreit, Llion Jones, Aidan N Gomez, Łukasz Kaiser, and Illia Polosukhin. Attention is all you need. *Advances in neural information processing systems*, 30, 2017.

- Yongqiang Wang, Abdelrahman Mohamed, Due Le, Chunxi Liu, Alex Xiao, Jay Mahadeokar, Hongzhao Huang, Andros Tjandra, Xiaohui Zhang, Frank Zhang, et al. Transformer-based acoustic modeling for hybrid speech recognition. In *IEEE International Conference on Acoustics, Speech and Signal Processing (ICASSP)*, pp. 6874–6878, 2020.
- Yongqiang Wang, Zhehuai Chen, Chengjian Zheng, Yu Zhang, Wei Han, and Parisa Haghani. Accelerating rnn-t training and inference using ctc guidance. In *Proc. ICASSP. IEEE*, 2023.
- Shinji Watanabe, Takaaki Hori, Suyoun Kim, John R Hershey, and Tomoki Hayashi. Hybrid ctc/attention architecture for end-to-end speech recognition. *IEEE Journal of Selected Topics in Signal Processing*, 11(8):1240–1253, 2017.
- Shinji Watanabe, Takaaki Hori, Shigeki Karita, Tomoki Hayashi, Jiro Nishitoba, Yuya Unno, Nelson Enrique Yalta Soplín, Jahn Heymann, Matthew Wiesner, Nanxin Chen, Adithya Renduchintala, and Tsubasa Ochiai. ESPnet: End-to-end speech processing toolkit. In *Proceedings of Interspeech*, pp. 2207–2211, 2018.
- Zhuoyuan Yao, Di Wu, Xiong Wang, Binbin Zhang, Fan Yu, Chao Yang, Zhendong Peng, Xiaoyu Chen, Lei Xie, and Xin Lei. WeNet: Production Oriented Streaming and Non-Streaming End-to-End Speech Recognition Toolkit. In *Proc. Interspeech*, pp. 4054–4058, 2021.
- Zhao You, Shulin Feng, Dan Su, and Dong Yu. 3m: Multi-loss, multi-path and multi-level neural networks for speech recognition. In *2022 13th International Symposium on Chinese Spoken Language Processing (ISCSLP)*, pp. 170–174. IEEE, 2022.
- Piotr Żelasko, Daniel Povey, Jan Trmal, Sanjeev Khudanpur, et al. Lhotse: a speech data representation library for the modern deep learning ecosystem. *arXiv preprint arXiv:2110.12561*, 2021.
- Binbin Zhang, Hang Lv, Pengcheng Guo, Qijie Shao, Chao Yang, Lei Xie, Xin Xu, Hui Bu, Xiaoyu Chen, Chenchen Zeng, et al. Wenetspeech: A 10000+ hours multi-domain mandarin corpus for speech recognition. In *IEEE International Conference on Acoustics, Speech and Signal Processing (ICASSP)*, pp. 6182–6186. IEEE, 2022a.
- Binbin Zhang, Di Wu, Zhendong Peng, Xingchen Song, Zhuoyuan Yao, Hang Lv, Lei Xie, Chao Yang, Fuping Pan, and Jianwei Niu. Wenet 2.0: More productive end-to-end speech recognition toolkit. *arXiv preprint arXiv:2203.15455*, 2022b.
- Frank Zhang, Yongqiang Wang, Xiaohui Zhang, Chunxi Liu, Yatharth Saraf, and Geoffrey Zweig. Faster, simpler and more accurate hybrid asr systems using wordpieces. *arXiv preprint arXiv:2005.09150*, 2020a.
- Qian Zhang, Han Lu, Hasim Sak, Anshuman Tripathi, Erik McDermott, Stephen Koo, and Shankar Kumar. Transformer transducer: A streamable speech recognition model with transformer encoders and rnn-t loss. In *IEEE International Conference on Acoustics, Speech and Signal Processing (ICASSP)*, pp. 7829–7833, 2020b.
- Ying Zhang, Mohammad Pezeshki, Philémon Brakel, Saizheng Zhang, Cesar Laurent Yoshua Bengio, and Aaron Courville. Towards end-to-end speech recognition with deep convolutional neural networks. *arXiv preprint arXiv:1701.02720*, 2017.

A APPENDIX

A.1 SCALEDADAM OPTIMIZER

A.1.1 SCALEDADAM ALGORITHM.

Algorithm 1 *ScaledAdam* Algorithm. RMS refers to root-mean-square function. g_t^2 refers to $g_t \odot g_t$. α_t is controlled by Eden learning rate schedule. Good default settings are $\beta_1 = 0.9$, $\beta_2 = 0.98$, $\eta = 0.1$, and $\epsilon = 10^{-8}$.

Require: learning rate α_t ; exponential decay rates for the moment estimates $\beta_1, \beta_2 \in [0, 1]$; scaling factor on the learning rate for parameter scale η ; objective function $f(\theta)$ with parameters θ ; initial parameter θ_0 .

```

t ← 0
m_0 ← 0, v_0 ← 0
n_0 ← 0, w_0 ← 0
r_0 ← RMS(θ_0)
while θ_t not converged do
  t ← t + 1
  g_t ← ∇_θ f_t(θ_{t-1})
  h_t ← g_t · θ_{t-1}
  r_{t-1} ← RMS(θ_{t-1})
  m_t = β_1 · m_{t-1} + (1 - β_1) · g_t
  v_t = β_2 · v_{t-1} + (1 - β_2) · g_t^2
  Δ'_t = -α_t · r_{t-1} · √(1-β_1^2) / (1-β_1^2) · m_t / √(v_t+ε)
  n_t ← β_1 · n_{t-1} + (1 - β_1) · h_t
  w_t ← β_2 · w_{t-1} + (1 - β_2) · h_t^2
  Δ'_{t,r} ← -η · α_t · √(1-β_2^2) / (1-β_1^2) · n_t / √(w_t+ε) ⊙ θ_{t-1}
  θ_t ← θ_{t-1} + Δ'_t + Δ'_{t,r}
end while

```

▷ Initialize step.
 ▷ Initialize first and second moment of parameter gradient.
 ▷ Initialize first and second moments of parameter scale gradient.
 ▷ Initialize parameter scale.
 ▷ Get parameter gradient.
 ▷ Get parameter scale gradient.
 ▷ Update the parameter scale.
 ▷ Update first moment of parameter gradient.
 ▷ Update second moment of parameter gradient.
 ▷ Compute parameter change.
 ▷ Update first moment of parameter scale gradient.
 ▷ Update second moment of parameter scale gradient.
 ▷ Compute parameter change by updating parameter scale.
 ▷ Update parameter.

A.1.2 COMPARISON BETWEEN SCALEDADAM AND ADAM.

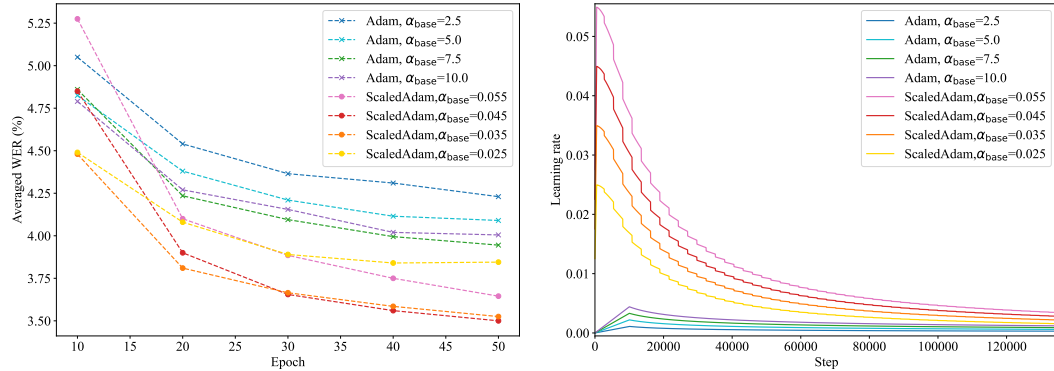
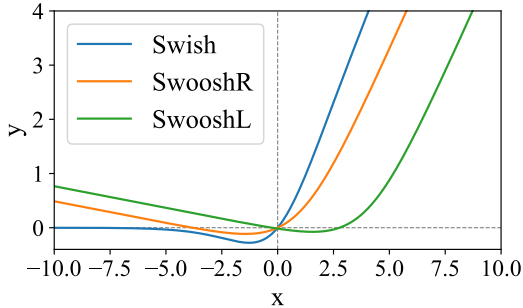


Figure A.2: Comparison between *ScaledAdam* and Adam in terms of: (Left) averaged WER on LibriSpeech *test-clean* and *test-other* at different epochs; (Right) learning rate at different steps.

A.2 ACTIVATION FUNCTIONS

Figure A.3: The activation functions: Swish, *SwooshR*, and *SwooshL*.

A.3 ACTIVATION CONSTRAINTS

Table 6: Ablation studies of activation constraints for *Zipformer-M* on LibriSpeech dataset. All models are trained for 40 epochs.

Ablation	test-clean (%)	test-other (%)
<i>Zipformer-M</i>	2.21	4.91
No <i>Balancer</i>	2.23	4.97
No <i>Whitener</i>	2.25	5.15
No <i>Balancer</i> , No <i>Whitener</i>	2.25	5.07

To ensure consistency in training and avoid badly trained modules, we propose the *Balancer* and the *Whitener*, which regularize the activations in a memory-efficient way. In forward pass, they are no-ops; in backward pass, they compute the gradients of the additional losses putting constraints on the activations \mathbf{g}' , and add that to the origin activation gradients \mathbf{g} : $\mathbf{g} = \mathbf{g} + \mathbf{g}'$. The placements of *Balancer* and *Whitener* may not seem to follow any very clear rules. They are generally applied when encountering specific instances of not-normally-trained models or model divergence. We first locate the abnormality to a specific module and then add the *Balancer* or *Whitener* to fix it.

A.3.1 BALANCER

Two failure modes commonly observed from the channel-wise statistical distribution are: **1**) the issue of activation values becoming excessively large or small can give rise to instability during the training process, particularly when employing mixed precision training; **2**) a significant number of “dead” neurons, whose outputs consistently remain negative, was observed upon examining the channel-wise statistics prior to the application of the non-linear activation function within the feed-forward modules. *Balancer* solves these issues by enforcing four constraints on each channel: lower and upper bounds of the mean value of absolute values, denoted as a_{\min} and a_{\max} ; minimum and maximum proportion of positive values, denoted as p_{\min} and p_{\max} respectively. Given the activation \mathbf{x} , intuitively we have $E[\mathbf{x}] \propto \lambda$, where λ represents the proportion of positive values. Due to the non-differentiable nature of positive value counting operation, a shifted version of Gaussian error function erf is introduced in order to approximate the mapping between $E[\mathbf{x}] \in (-\infty, \infty)$ and $\lambda \in [0, 1]$ by $2 \cdot \text{erf}(\mathbf{x}) - 1$, the inverse function of which can be approximated using $f_{\text{pos} \rightarrow E/\sqrt{\text{Var}}}(x) = \text{arctanh}(2x - 1)/(\sqrt{\pi} \cdot \log 2)$ without loss of generality. $\mu_{\min} = f_{\text{pos} \rightarrow E/\sqrt{\text{Var}}}(p_{\min})$ and $\mu_{\max} = f_{\text{pos} \rightarrow E/\sqrt{\text{Var}}}(p_{\max})$ can be further derived from the approximation. Following the same Gaussian assumption, the RMS is given by $\int_{-\infty}^{\infty} \frac{\sigma^2}{\sqrt{2\pi}} e^{-\frac{1}{2}(\mathbf{x}-\mu)^2} \text{abs}(\mathbf{x}) d\mathbf{x}$, where μ and σ^2 refer to the mean and variance of the Gaussian distribution. It can be approximated using $f_{\text{abs} \rightarrow \text{RMS}}(x) = \sqrt{\pi/2} \cdot x$ when $\mu \rightarrow 0$. Thus $r_{\min} = f_{\text{abs} \rightarrow \text{RMS}}(a_{\min})$ and $r_{\max} = f_{\text{abs} \rightarrow \text{RMS}}(a_{\max})$ can be further derived.

Specifically, the additional loss $\mathcal{L}_{\text{balancer}}$ conditioned on these constraints is defined as:

$$\begin{aligned}\mathcal{L}_{\text{RMS}} &= |\log(\min(\max(\text{RMS}[\mathbf{x}], r_{\text{max}}), r_{\text{min}})/\text{RMS}[\mathbf{x}])|, \\ \mathcal{L}_{\text{E}/\sqrt{\text{Var}}} &= |\text{E}[\mathbf{x}]/\sqrt{\text{Var}[\mathbf{x}]} - \text{clamp}(\text{E}[\mathbf{x}]/\sqrt{\text{Var}[\mathbf{x}]}, \mu_{\text{min}}, \mu_{\text{max}})|, \\ \mathcal{L}_{\text{balancer}} &= \mathcal{L}_{\text{RMS}} + \mathcal{L}_{\text{E}/\sqrt{\text{Var}}},\end{aligned}\tag{9}$$

where the statistics $\text{RMS}[\mathbf{x}]$, $\text{E}[\mathbf{x}]$, and $\sqrt{\text{Var}[\mathbf{x}]}$ are calculated in each channel. Before adding the additional gradient $\mathbf{g}' = \nabla_{\mathbf{x}}\mathcal{L}_{\text{balancer}}$ to the original activation gradient \mathbf{g} , \mathbf{g}' is scaled to $\mathbf{g}' = \mathbf{g}' \cdot \alpha/\text{RMS}[\mathbf{g}'] \cdot |\mathbf{g}|$. Herein, α is used to prevent \mathbf{g}' from overwhelming \mathbf{g} , and the per-element magnitude $|\mathbf{g}|$ is used to prevent the model from concentrating its “fixes” to the data distribution in frames with small gradients such as the padding frames. We set $\alpha = 0.04$ in this work.

A.3.2 WHITENER

Another failure mode on activations is that for the feature covariance, one or a few eigenvalues are dominating while others are extremely small. This tends to happen in a model that is about to diverge. *Whitener* encourages a more informative output distribution, by restricting the feature covariance after mean subtraction to have less unequal eigenvalues. Specifically, for output $\mathbf{x} \in \mathcal{R}^{N \times D}$ with N frames of D -dimensional features, we first compute the covariance matrix $C = (\mathbf{x} - \text{E}[\mathbf{x}])^T(\mathbf{x} - \text{E}[\mathbf{x}])$, where $C \in \mathcal{R}^{D \times D}$, and $\text{E}[\mathbf{x}]$ is per-channel mean. The auxiliary loss which measures the whiten metric $\mathcal{L}_{\text{whitener}}$ is defined as:

$$\mathcal{L}_{\text{whitener}} = (\sum_i \lambda_i^2/D)/(\sum_i \lambda_i/D)^2 = (\sum_i \sum_j C_{i,j}^2/D)/(\sum_i C_{i,i}/D)^2,\tag{10}$$

where $\boldsymbol{\lambda} = \{\lambda_1, \dots, \lambda_D\}$ are the eigenvalues of the covariance matrix C . To keep the original activation gradient \mathbf{g} dominant after adding the additional gradient $\mathbf{g}' = \nabla_{\mathbf{x}}\mathcal{L}_{\text{whitener}}$, \mathbf{g}' is scaled to $\mathbf{g}' = \mathbf{g}' \cdot \alpha/\ell^2(\mathbf{g}') \cdot \ell^2(\mathbf{g})$, where ℓ^2 denotes the L2 norm, and α is set to 0.01. The modification $\mathbf{g} = \mathbf{g} + \mathbf{g}'$ is done only when the whiten metric $\mathcal{L}_{\text{whitener}}$ is above a certain value w_{min} to prevent the model from learning pathological activation distributions. We usually set w_{min} to 10.

A.3.3 ABLATION STUDIES.

We perform ablation experiments on LibriSpeech dataset to validate the effect of *Balancer* and *Whitener*. Table 6 presents the experimental results. All models are trained for 40 epochs. Removing *Balancer* does not lead to obvious change on model performance. However, it would increase the risk of model divergence without the value range constraints especially when employing mixed precision training. Removing *Whitener* results in 0.04% and 0.24% WER reduction on *test-clean* and *test-other*, respectively. This indicates that restricting the feature covariance to have less unequal eigenvalues in *Whitener* can boost performance.

A.4 EXPERIMENTS ON LIBRISPEECH DATASET

A.4.1 TRAINING CONFIGURATIONS OF ZIPFORMER MODELS

Before training, the Mel filter-bank features are pre-computed and saved to disk. In training, we use *DynamicBucketingSampler* in Lhotse toolkit (Zelasko et al., 2021) to form the batches, where the batch size is determined dynamically given the constraint of the maximum total speech duration (in seconds). Table 7 presents the training configurations of *Zipformer* models on LibriSpeech dataset with speed perturbation with factors of 0.9, 1.0, and 1.1.

A.4.2 COMPARISON WITH STATE-OF-THE-ART MODELS

As an extension of Table 2, Table 8 adds the results on LibriSpeech dataset for *Zipformer* with CTC and CTC/AED architectures respectively. For the *Zipformer* CTC/AED model, we use a 6-layer Transformer as AED decoder, each layer with attention dimension of 512, attention heads number of 8, and feed-forward hidden dimension of 2048. The *Zipformer* CTC models are trained for 100 epochs while the *Zipformer* CTC/AED models are trained for 50 epochs. Detailed training configurations are provided in Section A.4.1.

Table 7: Training configurations of *Zipformer* models on LibriSpeech dataset.

Model	Type	Params (M)	Max duration (s)	GPUs	Epochs	Training time / epoch (m)
<i>Zipformer</i> -S	CTC	22.1	1700	2 32G Tesla V100	100	86
<i>Zipformer</i> -M	CTC	64.3	1400	4 32G Tesla V100	100	60
<i>Zipformer</i> -L	CTC	147.0	1200	4 32G Tesla V100	100	76
<i>Zipformer</i> -S	CTC/AED	46.3	1700	2 32G Tesla V100	50	105
<i>Zipformer</i> -M	CTC/AED	90.0	1200	4 32G Tesla V100	50	67
<i>Zipformer</i> -L	CTC/AED	174.3	1200	4 32G Tesla V100	50	84
<i>Zipformer</i> -S	pruned transducer	23.3	1500	2 32G Tesla V100	50	87
<i>Zipformer</i> -M	pruned transducer	65.6	1000	4 32G Tesla V100	50	69
<i>Zipformer</i> -L	pruned transducer	148.4	1000	4 32G Tesla V100	50	80
<i>Zipformer</i> -L	pruned transducer	148.4	2200	8 80G Tesla A100	200	18

For the CTC systems, *Zipformer*-M outperforms Squeezeformer-ML on both test sets with only about half the number of parameters, and *Zipformer*-L also surpasses Squeezeformer-L by 0.27% on *test-other* with fewer parameters. For CTC/AED systems, *Zipformer*-M outperforms Conformer models and Branchformer, while *Zipformer*-L achieves comparable results with E-Branchformer-L. Note that as presented in Figure 3, *Zipformer*-L is much more efficient than E-Branchformer-L.

Table 8: WER(%) comparison between different models on LibriSpeech dataset. We also include the number of parameters and FLOPs of encoder for a 30s input audio measured with DeepSpeed (Rasley et al., 2020). *Trained with 8 80G NVIDIA Tesla A100 GPUs for 170 epochs.

Model	Type	Params (M)	GFLOPs	<i>test-clean</i> (%)	<i>test-other</i> (%)
Squeezeformer-XS (Kim et al., 2022)	CTC	9.0	18.2	3.74	9.09
Squeezeformer-S (Kim et al., 2022)	CTC	18.6	33.7	3.08	7.47
Squeezeformer-SM (Kim et al., 2022)	CTC	28.2	47.6	2.79	6.89
Squeezeformer-M (Kim et al., 2022)	CTC	55.6	88.4	2.56	6.50
Squeezeformer-ML (Kim et al., 2022)	CTC	125.1	183.3	2.61	6.05
Squeezeformer-L (Kim et al., 2022)	CTC	236.3	333.7	2.47	5.97
E-Branchformer-B (Kim et al., 2023)	CTC/AED	41.1	78.1	2.49	5.61
Branchformer (Peng et al., 2022)	CTC/AED	116.2	238.3	2.4	5.5
E-Branchformer-L (Kim et al., 2023)	CTC/AED	148.9	284.4	2.14	4.55
Conformer-S (Gulati et al., 2020)	transducer	10.3	–	2.7	6.3
Conformer-M (Gulati et al., 2020)	transducer	30.7	–	2.3	5.0
Conformer-L (Gulati et al., 2020)	transducer	118.8	–	2.1	4.3
Conformer in WeNet (Zhang et al., 2022b)	CTC/AED	121.3	–	2.66	6.53
Conformer in ESPnet (Miyazaki et al., 2023)	CTC/AED	113.2	–	2.29	5.13
Conformer-S	pruned transducer	9.8	29.1	3.75	9.24
Conformer-M	pruned transducer	28.4	77.0	2.96	7.11
Conformer-L	pruned transducer	122.5	294.2	2.46	5.55
<i>Zipformer</i> -S	CTC	22.1	40.8	2.85	6.91
<i>Zipformer</i> -M	CTC	64.3	62.9	2.51	6.02
<i>Zipformer</i> -L	CTC	147.0	107.7	2.49	5.7
<i>Zipformer</i> -S	CTC/AED	46.3	40.8	2.46	6.04
<i>Zipformer</i> -M	CTC/AED	90.0	62.9	2.22	4.97
<i>Zipformer</i> -L	CTC/AED	174.3	107.7	2.09	4.59
<i>Zipformer</i> -S	pruned transducer	23.3	40.8	2.42	5.73
<i>Zipformer</i> -M	pruned transducer	65.6	62.9	2.21	4.79
<i>Zipformer</i> -L	pruned transducer	148.4	107.7	2.06	4.63
<i>Zipformer</i> -L*	pruned transducer	148.4	107.7	2.00	4.38